



The 25<sup>th</sup> Iranian Conference on  
Optics and Photonics (ICOP 2019),  
and the 11<sup>th</sup> Iranian Conference on  
Photonics Engineering and  
Technology (ICPET 2019).  
University of Shiraz,  
Shiraz, Iran,  
Jan. 29-31, 2019



## اثر کاتیون سزیم بر عملکرد سلول خورشیدی پروسکایتی با جاذب $\text{CH}_3\text{NH}_3\text{PbI}_3$

نسرین صلح طلب<sup>۱</sup>، وحید احمدی<sup>۱\*</sup>، فرزانه عربپور رق آبادی<sup>۱</sup>، بهرام عبدالحی نژاد<sup>۱</sup>

<sup>۱</sup> ایران، تهران، دانشگاه تربیت مدرس، دانشکده مهندسی برق و کامپیوتر، گروه پژوهشی ایتوالکترونیک و نانوفوتونیک

<sup>۲</sup> ایران، تهران، دانشگاه تربیت مدرس، دانشکده مهندسی شیمی، گروه فرایند

\*نویسنده مسئول: [V\\_ahmadi@modares.ac.ir](mailto:V_ahmadi@modares.ac.ir)

**چکیده** - در این پژوهش برای بهبود عملکرد سلول خورشیدی پروسکایتی، لایه جاذب متیل آمونیوم سرب یدید با کاتیون سزیم مخلوط می شود. خواص نوری، مورفولوژی و ساختار کریستالی فیلم پروسکایتی در حضور غلظت های مختلف از کاتیون سزیم مورد بررسی قرار می گیرد. لایه پروسکایت با یکنواختی بیشتر در حضور سزیم با غلظت ۰.۰۵ مولار بدست می آید که سلول خورشیدی با بالاترین بازده را نیز نتیجه می دهد.

**کلید واژه** - سلول خورشیدی، سزیم، جاذب پروسکایتی

## The effect of Cs cation on the performance of $\text{CH}_3\text{NH}_3\text{PbI}_3$ perovskite solar cell

Nasrin Solhtalab<sup>1</sup>, Vahid Ahmadi<sup>1</sup>, Farzaneh Arabpour Roghabadi<sup>1,2</sup>

,Bahram Abdolahi Najand<sup>1</sup>

<sup>1</sup> Optoelectronic and Nanophotonic Research Group, Faculty of Electrical and Computer Engineering, Tarbiat Modares University, Tehran-Iran.

<sup>2</sup> Faculty of Chemical Engineering, Tarbiat Modares University, Tehran, Iran

\*Corresponding author: [v\\_ahmadi@modares.ac.ir](mailto:v_ahmadi@modares.ac.ir)

**Abstract**- In this work, methylammonium lead iodide ( $\text{CH}_3\text{NH}_3\text{PbI}_3$ ) perovskite light absorbers are doped by cesium to improve the performance of perovskite solar cell. The optical, morphological, and crystalline properties of the pure and mixed perovskite films are investigated. The most uniform perovskite layer is obtained for the film containing 0.05M of CsCl that yields the device with higher power conversion efficiency (4.64%) than the other concentrations.

**Keywords:** Perovskite solar cell; Cesium, Perovskite absorber

## 1. Introduction

Perovskite solar cells have attracted enormous interest in recent years due to the rapid growth of the power conversion efficiencies (PCE) from 3.8% in 2009 [1] to the current world record of 22.0% [2]. The organic-inorganic perovskite material has an ABX<sub>3</sub> structure and is typically comprised of an organic cation, A=methylammonium (MA) CH<sub>3</sub>NH<sub>3</sub><sup>+</sup>; formamidinium (FA) CH<sub>3</sub>(NH<sub>2</sub>)<sub>2</sub><sup>+</sup>, a divalent metal, B = (Pb<sup>2+</sup>; Sn<sup>2+</sup>), and an anion X = (Cl<sup>-</sup>; Br<sup>-</sup>; I<sup>-</sup>). The perovskite material can be processed by various techniques including spin coating, dip coating, 2-step interdiffusion, chemical vapour deposition, thermal evaporation, that introduce perovskite solar cell as one of the most versatile photovoltaic (PV) technologies. The achieved high performances for perovskite solar cells have been attributed to exceptional material properties such as remarkably high absorption over the visible spectrum, low exciton binding energy, charge carrier diffusion lengths in the μm-range, a sharp optical band edge, and a tunable band gap from 1.1 to 2.3 eV by interchanging the above cations, metals, and/or halides [3]. One of the main strategies that are used to tune the optical and electrical properties, enhance the stability, and improve the performance of the perovskite devices is employing mixed halide, cations, and metals sites in the crystalline structure. In this work, CH<sub>3</sub>NH<sub>3</sub>PbI<sub>3</sub> perovskite is doped with Cs cation and used as the absorber layer of the perovskite device. The optical and structural properties of the absorber is characterized in the presence of Cs. Furthermore, the perovskite devices based on the doped absorber are fabricated and characterized.

## 2. Experimental Section

To fabricate solar cells, fluorine-doped tin oxide (FTO) substrates are patterned by an HCl solution (2 M in deionized water) and Zn powder. Then the etched substrates are ultra-sonicated in deionized water, acetone, ethanol, and isopropanol, each for 10 min, followed by drying at 100 °C, and subsequently treated by UV-ozone for 15 min. The

cleaned FTO substrates are coated with a compact layer of TiO<sub>2</sub> by spin coating of a mild acidic solution of tetraisopropyl orthotitanate in ethanol (2000 RPM for 30 s), followed by annealing at 500 °C for 30 min. The mesoporous TiO<sub>2</sub> layer is deposited on the TiO<sub>2</sub> compact layer by spin coating (5000 RPM for 30 s) of the TiO<sub>2</sub> paste containing 20-nm-sized TiO<sub>2</sub> nanoparticles diluted in ethanol (2:7 weight ratio), and immediately dried at 70 °C for 30 min. Then, perovskite layer is deposited on the mesoporous TiO<sub>2</sub> layer. A poly(3 hexylthiophene)(P3HT layer (10 mg/mL in anhydrous chlorobenzene) is spin-coated on the perovskite layer at 2000 RPM for 60 s. Finally, a 100-nm-thick Au cathode is deposited on it by a thermal evaporator with a shadow mask (Nanostructured Coatings Co, Iran).

In order to synthesize the perovskite absorber layer, one step solution method is used. CsCl, MAI, and PbI<sub>2</sub> are dissolved into a mixed solvent of DMF: DMSO (4 : 1, volume ratio). As CsCl is difficultly dissolved in the solvent mixture, the solution is heated at 70 °C for 24 h. The perovskite films are prepared with different CsCl concentration that are 0, 0.05, 0.1, and 0.2 M. 30μL of freshly prepared perovskite solutions was spin-coated on the mesoporous TiO<sub>2</sub> layer at 4000 rpm for 20 s. After a 4 s delay time of the spin coating process, a 240 μL of anhydrous chlorobenzene was quickly dropped at the substrate. then dried at 100 °C for 10 min. The colour of the annealed film changed from transparent to dark brown indicating the crystallization of the perovskite layer.

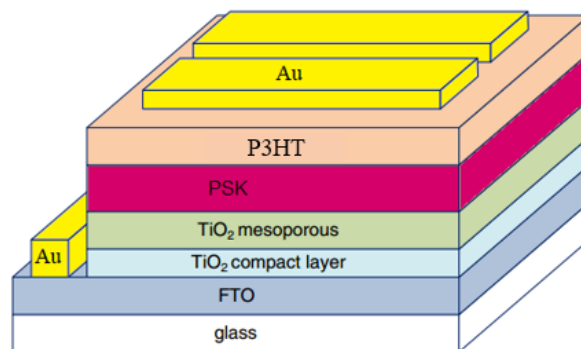


Figure 1 Schematic of the fabricated device structure.

### 3. Results and discussions

The SEM images of the surface of the deposited perovskite layers containing different amount of CsCl (0, 0.05, 0.1, 0.2 molar). in the precursor are presented in Figure 2.

As observed, more uniform layer is achieved when the concentration of CsCl in the precursor is 0.05M. Interestingly, the amount of the holes in this layer is fewer than the other films.

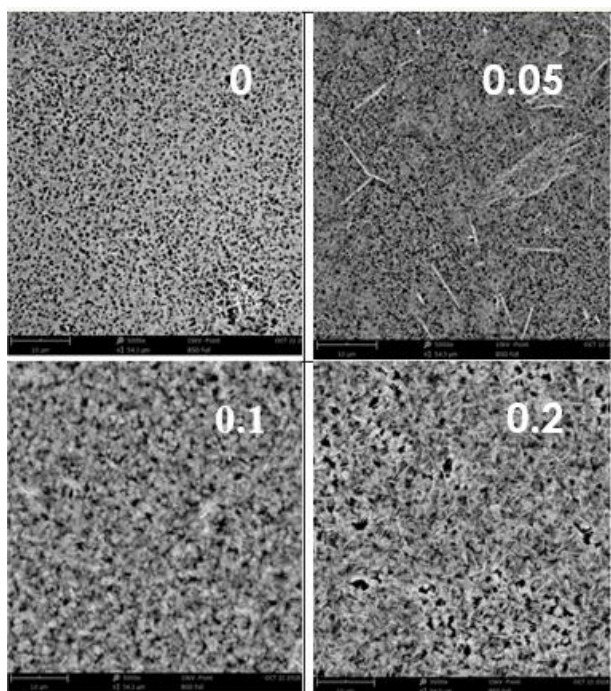


Figure 2 SEM images of the surface of the perovskite films comprising different concentrations of CsCl in the precursor solution (0, 0.05, 0.1, 0.2 molar).

To gain insight on the effect of Cs-substitution on the crystallization of the MAPbI<sub>3</sub> perovskite, a series of perovskite films with different Cs content are characterized using X-ray diffraction (XRD). Figure 3a shows the XRD patterns of Cs<sub>x</sub>MA<sub>1-x</sub>PbI<sub>3</sub> perovskite films with different Cs content. The sharp peaks located at 14.23, 28.57, 32 ° are attributed to (110), (220), (310) planes of the tetragonal structure of the perovskite, respectively. For clarity, Figure 3b shows a high resolution view of the (110) diffraction peak of the MA<sub>1-x</sub>Cs<sub>x</sub>PbI<sub>3</sub> samples. The peak location monotonically shifts from 14.23° to 14.29° with increasing CsCl content from 0 to 0.2 M due to the smaller Cs<sup>+</sup> radius (1.81 Å) compared to that of MA<sup>+</sup> (2.70 Å). It

demonstrates that Cs cations are effectively integrated into the MAPbI<sub>3</sub> perovskite lattice and the increased intensity of the  $\delta$ -phase CsPbI<sub>3</sub> indicates a substitution limit. This non-provskite yellow phase can lead the reduction of the PCE of the device.

(a)

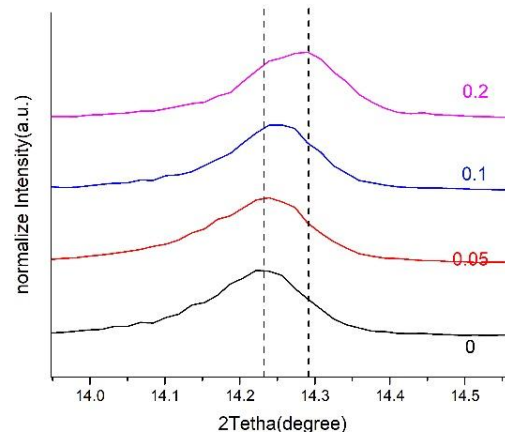
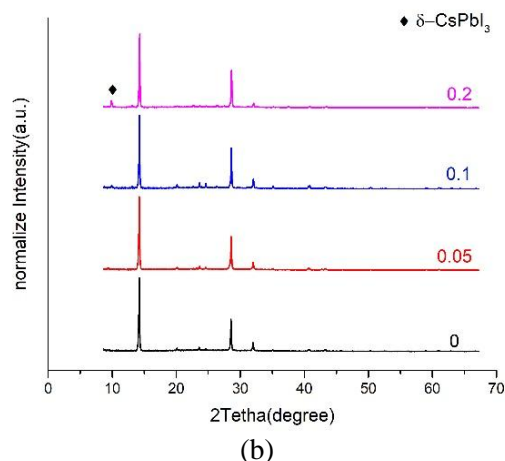


Figure 3 (a) XRD spectra of the perovskite films comprising different concentrations of CsCl in the precursor solution, and (b) a high resolution view of the (110) diffraction peak of the MA<sub>1-x</sub>Cs<sub>x</sub>PbI<sub>3</sub> samples.

The UV-Vis spectra of the pure and mixed perovskite films indicate an initial blue-shift of the absorption edge shown in Figure 4, occurs due to the Cs content enhancement.

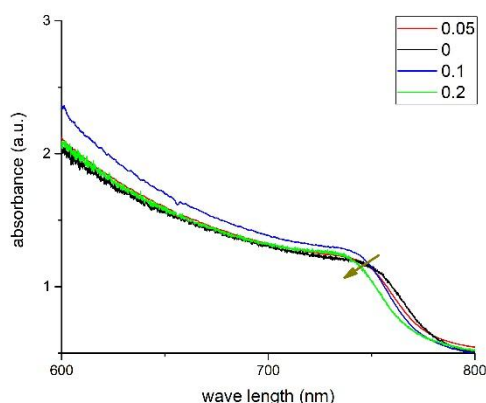


Figure 4 Visible spectra of the pure and mixed perovskite films.

Figure 5, shows the forward and backward current density-voltage characteristics of the devices with different concentrations of CsCl in the precursor solution. The best performance is achieved for the device comprising 0.05 M cesium chloride. This device yields a PCE of 4.64%.

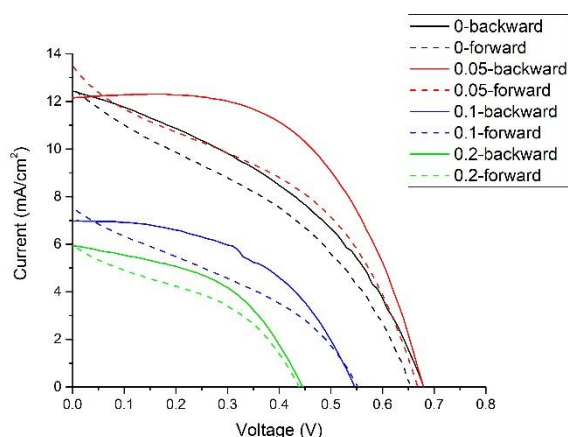


Figure 5 J-V characteristics of the devices including different perovskite layers.

Table 1 summarizes the photovoltaic performance of the devices with different percentages of cesium chloride.

**Table 1 Photovoltaic performance of the perovskite devices.**

Device	Voc	Isc	PCE	FF
0	0.66	11.2	3.21	0.43
0.05	0.68	12.15	4.64	0.56
0.1	0.55	6.97	1.87	0.48
0.2	0.45	5.94	1.25	0.46

## Conclusion

In summary, the effect of the presence of CsCl on the crystalline, optical, and morphology of the  $\text{CH}_3\text{NH}_3\text{PbI}_3$  perovskite films were investigated. It was shown that among all concentrations of CsCl, the best performance was achieved for the device with 0.05 M CsCl in the perovskite precursor solution.

## Acknowledgements

The authors would like to acknowledge the financial support from the research department of Tarbiat Modares University (Research group of nano plasma photonic, IG-39704).

## References

- [1] A. Kojima, K. Teshima, Y. Shirai, and T. J. J. o. t. A. C. S. Miyasaka, "Organometal halide perovskites as visible-light sensitizers for photovoltaic cells," vol. 131, no. 17, pp. 6050-6051, 2009.
- [2] W. S. Yang *et al.*, "Iodide management in formamidinium-lead-halide-based perovskite layers for efficient solar cells," vol. 356, no. 6345, pp. 1376-1379, 2017.
- [3] W. S. Yang *et al.*, "High-performance photovoltaic perovskite layers fabricated through intramolecular exchange," vol. 348, no. 6240, pp. 1234-1237, 2015.